Currents on conducting surfaces of a semiellitpical-channel-backed slotted screen in an isorefractive environment

Danilo Erricolo, *Senior Member, IEEE*, Michael D. Lockard, *Student Member, IEEE*, Chalmers M. Butler, *Life Fellow, IEEE*, Piergiorgio L. E. Uslenghi, *Fellow, IEEE*

Abstract— **Electromagnetic penetration through an aperture into a cavity is considered. The structure of interest is a semielliptical channel flush-mounted under a metal plane and slotted along the interfocal distance of its cross-section. The channel is filled with a material isorefractive to the medium that occupies the half-space above the metal plane. Three independent integral equations are developed to compute the currents induced on the structure of interest by plane wave and line source excitations. Numerical results from the integral equation methods are compared with the evaluation of the analytical expressions, derived in a previous paper, that involve the summation of Mathieu functions. Data are presented for two polarizations, various values of intrinsic impedances and ratio between aperture width and incident radiation wavelength. Further data are presented for the bistatic radar cross-section of the structure of interest. All data obtained from the integral equation methods and the evaluations of the analytical formulas provide excellent agreement.**

Keywords— **Electromagnetic radiation, electromagnetic scattering, complex media, integral equation, Mathieu function, aperture penetration, numerical solutions, isorefractive media.**

I. Introduction

TWO different methods are considered for determining the currents on the structure illustrated in Fig. 1, which depicts a slotted conducting plane backed by a semielliptical cavity with conducting walls. Fig. 1 shows a two-dimensional structure in which the media are isorefractive and the excitation may be a $z-$independent plane wave or line source in the exterior region or a $z-$independent line source in the interior region.

One method to obtain the currents induced on the structure of Fig. 1 is through the evaluation of the numerical solutions of integral equations, described in Section II. Another method is through the evaluation of the analytic expression derived by Uslenghi [1]. The goal of this work is to obtain two independent solutions for the currents on the structure of Fig. 1 and to compare the numerical results of the two methods.

This work continues and completes the comparisons started in [2]. Since analytic expressions for the electromagnetic fields exist, one may look upon this problem as canonical, yet it is by no means a simple problem because the structure comprises a cavity, sharp edges, and two isorefractive media, which prompts one to expect a field with varied features.

Initially the authors sought numerical results from the analytic solution of [1] to establish a benchmark for numerical solutions. However, the difficulties in the evaluations of the analytic solution, whose constituent components are expressed as infinite series of Mathieu functions that may be slowly convergent for some combinations of the various parameters, led to a mutual validation of independent solution methods.

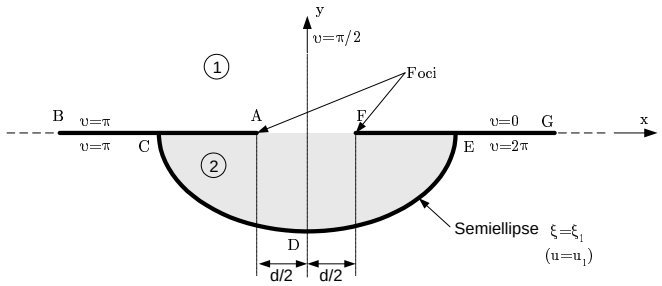

Fig. 1. Cross section of the two-dimensional geometry. Two half planes, AB and FG originate at the foci A and F of an elliptic coordinate system with focal distance d. Regions 1 and 2 are coupled through the aperture or slot AF. Region 2 is a cavity limited by the baffles AC, EF and by the metallic semielliptical wall CDE, located at the elliptic coordinate ξ_1 or (u_1).

The geometry of this problem is most easily described in the elliptic coordinates (u, v) related to the Cartesian coordinates by $x = d/2 \cosh u \cos v$ and $y = d/2 \sinh u \sin v$. It is also convenient to introduce another pair of elliptic coordinates defined as $\xi = \cosh u$ and $\eta = \cos v$. The materials in region 1 and 2 of Fig. 1 are isorefractive, *i.e.*, the dielectric permittivities $\varepsilon_1, \varepsilon_2$ and permeabilities μ_1, μ_2 are such that $\varepsilon_1\mu_1 = \varepsilon_2\mu_2$, which implies equal wavenumbers $k_1 = \omega\sqrt{\varepsilon_1\mu_1} = \omega\sqrt{\varepsilon_2\mu_2} = k_2$ and, in general, unequal intrinsic impedances $Z_1 = \sqrt{\mu_1/\varepsilon_1} \neq \sqrt{\mu_2/\varepsilon_2} = Z_2$.

The behavior of the induced current on all conducting surfaces of the structure is examined for different excita-

This work was supported by the U.S. Department of Defense and the US Air Force Office of Scientific Research under MURI grant F49620-01-1-0436 and under DURIP grant F49620-02-1-0440. Additionally, this work was supported in part by a grant of computer time from the DOD High Performance Computing Modernization Program at ASC. The authors would also like to acknowledge the support of the National Defense Science and Engineering Graduate Fellowship. D. Erricolo and P. L. E. Uslenghi are with the Department of Electrical and Computer Engineering, University of Illinois at Chicago, Chicago, IL 60607 USA. Email: erricolo@ece.uic.edu, uslenghi@uic.edu. M. D. Lockard and C. M. Butler are with the Holcombe Department of Electrical and Computer Engineering, Clemson University, Clemson, SC 29634-0915 USA. Email: mlockar@mail.clemson.edu, chalmers.butler@ces.clemson.edu.

tions: plane wave, line source outside the cavity, and line source inside the cavity. Two polarizations are considered. Results are provided for different values of the impedances of the two isorefractive materials and also for different values of the ratio between the aperture width and the wavelength of the incident radiation. Further results are provided for the bistatic radar cross section of the structure of Fig. 1. Details of the computation of Mathieu functions and series of them are found in [3]. The integral equation methods discussed are more general than the analytical formulas in that the former are not limited to the semielliptic backing and isorefractive media. The agreement among the numerical results for the current determined by these different methods is excellent in all cases considered.

II. DETERMINATION OF SURFACE CURRENTS FROM INTEGRAL EQUATION SOLUTIONS

Three different integral equation methods to compute currents induced on the structure of Fig. 1 are discussed in this section. A coupled integral equation method is discussed for each polarization followed by a single integral equation scatterer method that utilizes a finite-width groundplane. The scatterer method provides further validation of the data presented for the TM-polarized case and also provides insight into the relationship between equivalent currents and actual currents. The time-dependence factor $exp(+j\omega t)$ is omitted throughout.

A. Coupled Integral Equations (TE)

Coupled integral equations are formulated and solved for equivalent currents, which produce the same total fields in the two regions of Fig. 2 as exist in the original structure [2], [4]. These equivalent currents are known and are used to compute the z-directed component of the total magnetic field, which is directly related to the actual current present on the surfaces of the structure in Fig. 1.

$M_{z(x)}$ and $J_{l(z)}$ of Fig. 2 are equivalent currents whose values are known from [2]. The coordinates of the endpoints of the aperture are x_1 and x_2 and the contour of the channel backing and its image is denoted by C_s^i.

The current on the surface of the ground plane in region 1 of Fig. 1 is given by

$$\mathbf{J}_x^{BA} = (\widehat{\mathbf{y}} \times \widehat{\mathbf{z}})\, H_z^1(x,0)\big|_{BA} = \widehat{\mathbf{x}}\, H_z^1(x,0)\big|_{BA} \qquad (1)$$

$$\mathbf{J}_x^{FG} = (\widehat{\mathbf{y}} \times \widehat{\mathbf{z}}) H_z^1(x,0)\big|_{FG} = \widehat{\mathbf{x}}\, H_z^1(x,0)\big|_{FG}, \qquad (2)$$

where

$$H_z^1(x,0) = H_z^{sc}(x,0) + \mathcal{H}_z^1[2M_z; x, 0] \qquad (3)$$

with

$$\mathcal{H}_z^1[M_z; x, 0] = \int_{x_1}^{x_2} M_z(x')\, G^A(x,0;x',0;k_1,\eta_1)\, dx'. \qquad (4)$$

For plane wave excitation,

$$H_z^{sc}(x) = 2e^{jk_1(x\cos\phi_o)}, \qquad (5)$$

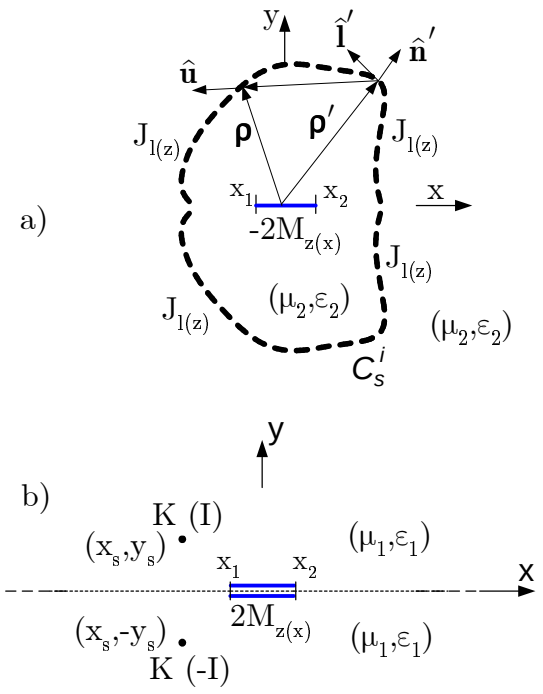

Fig. 2. Equivalent models for TE (TM) coupled integral equations method: a) Interior equivalent model, b) exterior equivalent model. Quantities in parenthesis are associated with TM-polarization.

where φ_0 is the angle between the direction of the incident wavevector and the negative x-axis. For line source excitation,

$$H_z^{sc}(x) = 2KG^A(x,0;x_s,y_s;k_1,\eta_1), \qquad (6)$$

where K is the strength of the impressed magnetic line source. The Green's function in these expressions is that of a magnetic line source in free space,

$$G^A(x,y;x',y';k,\eta) = -\frac{k}{4\eta} H_0^{(2)}\left(k\sqrt{(x-x')^2+(y-y')^2}\right). \qquad (7)$$

Similarly, the current on the surface of the ground plane that is in region 2 is given by

$$\mathbf{J}_x^{CA} = (-\widehat{\mathbf{y}} \times \widehat{\mathbf{z}})\, H_z^2(x,0)\big|_{CA} = -\widehat{\mathbf{x}}\, H_z^2(x,0)\big|_{CA} \qquad (8)$$

$$\mathbf{J}_x^{FE} = (-\widehat{\mathbf{y}} \times \widehat{\mathbf{z}})\, H_z^2(x,0)\big|_{FE} = -\widehat{\mathbf{x}}\, H_z^2(x,0)\big|_{FE} \qquad (9)$$

where

$$H_z^2(x,y) = \mathcal{H}_z^2[-2M_z; x, y] + \mathcal{H}_z^2[J_l; x, y] \qquad (10)$$

with

$$\mathcal{H}_z^2[-2M_z; x, y] = \int_{x_1}^{x_2} 2M_z(x')\, G^A(x,y;x',0;k_2,\eta_2)\, dx' \qquad (11)$$

and

$$\mathcal{H}_z^2[J_l; x, y] = \int_{C_s^i} J_l(x',y')\, G^B(x,y;x',y';k_2)\, dl'. \qquad (12)$$

The Green's function in (12) is defined as

$$G^B(x,y;x',y';k) = -\frac{k}{4j}\cos(\theta')\times H_1^{(2)}\left(k\sqrt{(x-x')^2+(y-y')^2}\right) \quad (13)$$

where

$$\cos\theta' = \hat{\mathbf{u}}\bullet\hat{\mathbf{n}}' \ , \quad \hat{\mathbf{u}} = \frac{\rho-\rho'}{|\rho-\rho'|} \quad , \quad \hat{\mathbf{n}}' = \hat{\mathbf{l}}'\times\hat{\mathbf{z}} \ ,$$

and the vectors $\hat{\mathbf{u}}$, $\hat{\mathbf{n}}'$, and $\hat{\mathbf{l}}'$ are illustrated in Fig. 2. It should be noted that the equivalent models, unlike the original structure, yield a total magnetic field that is continuous and nonsingular through the x axis and so the field evaluations along $x = 0$ do not require one to take the limit from the appropriate side of the ground plane.

The current on the surface CDE is identical to the equivalent current J_l because the field is zero in the lower half-space outside of the semiellipse $\xi = \xi_1$ and the total magnetic field must be discontinuous by the value of the equivalent electric current, *i.e.*

$$\mathbf{J}_\ell = -\hat{\mathbf{n}}\times\hat{\mathbf{z}}\left[H_z^2\big|_{\xi_1^-} - H_z^2\big|_{\xi_1^+}\right] = \hat{\ell}\,H_z^2\big|_{\xi_1^-} = \mathbf{J}_\ell^{CDE}, \quad (14)$$

where ξ_1^- is the contour on the inside surface of the semiellipse, and ξ_1^+ is on the outside surface of the semiellipse.

The known equivalent currents M_z and J_l are represented by pulses and equations (3) and (10) are evaluated at discrete points to obtain values for the total magnetic field. The results are substituted into equations (1), (2), (8), and (9) to obtain the actual currents present on the original structure.

B. Coupled Integral Equations (TM)

The current present on the surfaces of the structure of Fig. 1 is determined from the equivalent current obtained from the coupled integral equations method for TM excitation. The equivalent currents are used to determine the x-directed component of the total magnetic field in both regions of Fig. 2. The total magnetic field is then related to the z-directed electric current on the PEC surfaces.

The current on the surface of the ground plane in region 1 of Fig. 1 is given by

$$\mathbf{J}_z^{BA} = (\hat{\mathbf{y}}\times\hat{\mathbf{x}})\,H_x^1(x,0)\big|_{BA} = -\hat{\mathbf{z}}\,H_x^1(x,0)\big|_{BA} \quad (15)$$

and

$$\mathbf{J}_z^{FG} = (\hat{\mathbf{y}}\times\hat{\mathbf{x}})\,H_x^1(x,0)\big|_{FG} = -\hat{\mathbf{z}}\,H_x^1(x,0)\big|_{FG} \ , \quad (16)$$

where

$$H_x^1(x,0) = H_x^M\left[2M_x(x');k_1;x\right] + H_x^{SC}(x) \ , \quad (17)$$

$$H_x^M\left[M_x(x');k;x\right] = -\frac{1}{4k\eta}\times \left(k^2+\frac{\partial^2}{\partial x^2}\right)\int_{x_1}^{x_2} M_x(x')\,H_0^{(2)}(k|x-x'|)\,dx' \ , \quad (18)$$

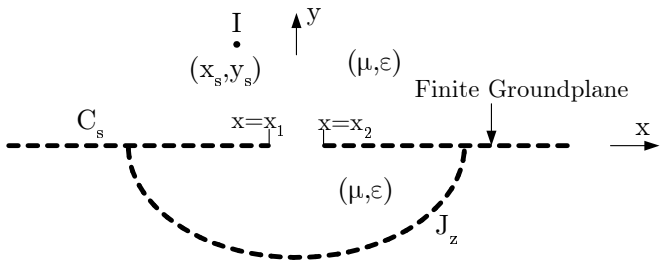

Fig. 3. Equivalent model for the scatterer method.

$$H_x^{SC}(x) = -\frac{2}{\eta_1}\sin\phi_o e^{jk_1x\cos\phi_o} \quad (19)$$

for plane wave excitation, and

$$H_x^{SC}(x) = \frac{Ik_1}{2j}\frac{y_s}{\sqrt{(x-x_s)^2+y_s^2}}\times H_1^{(2)}\left(k_1\sqrt{(x-x_s)^2+y_s^2}\right) \quad (20)$$

for line source excitation, where I is the strength of the impressed electric line source. Evaluation of equation (18) is required in solving the coupled integral equations, and subroutines for determining the fields can easily be adapted from these existing codes. One also notes that the kernel is not singular where (18) is to be evaluated, *i.e.*, the source points are located at the aperture and the observation points are placed everywhere along $y = 0$ *except* at the aperture. The current present on the ground plane surface in region 2 is given by

$$\mathbf{J}_z^{CA} = (-\hat{\mathbf{y}}\times\hat{\mathbf{x}})\,H_x^2(x,0)\big|_{CA} = \hat{\mathbf{z}}\,H_x^2(x,0)\big|_{CA} \quad (21)$$

and

$$\mathbf{J}_z^{FE} = (-\hat{\mathbf{y}}\times\hat{\mathbf{x}})\,H_x^2(x,0)\big|_{FE} = \hat{\mathbf{z}}\,H_x^2(x,0)\big|_{FE} \ , \quad (22)$$

where

$$H_x^2(x,0) = H_x^M\left[-2M_x(x');k_2;x\right] + H_x^J\left[J_z(x',y');k_2;x\right] \ , \quad (23)$$

$H_x^M\left[-2M_x(x');k;x\right]$ is given in (18), and

$$H_x^J\left[J_z(x',y);k;x\right] = \frac{k}{4j}\times \int_{C_S^i} J_z(x',y')\frac{y'H_1^{(2)}\left(k\sqrt{(x-x')^2+y'^2}\right)}{\sqrt{(x-x')^2+y'^2}}dl'. \quad (24)$$

The variable ℓ' in (24) is the displacement along the contour C_S^i. The current on the surface CDE is identical to the equivalent current J_z because the fields are zero in the lower half-space outside of the semiellipse and the component of the total magnetic field that is tangential to the semielliptical surface must be discontinuous by the value of the equivalent electric current, *i.e.*,

$$\mathbf{J}_z = -\hat{\mathbf{n}}\times\hat{\mathbf{l}}\left[H_l^2\big|_{\xi_1^-} - H_l^2\big|_{\xi_1^+}\right] = -\hat{\mathbf{z}}\,H_l^2\big|_{\xi_1^-} = \mathbf{J}_z^{CDE}. \quad (25)$$

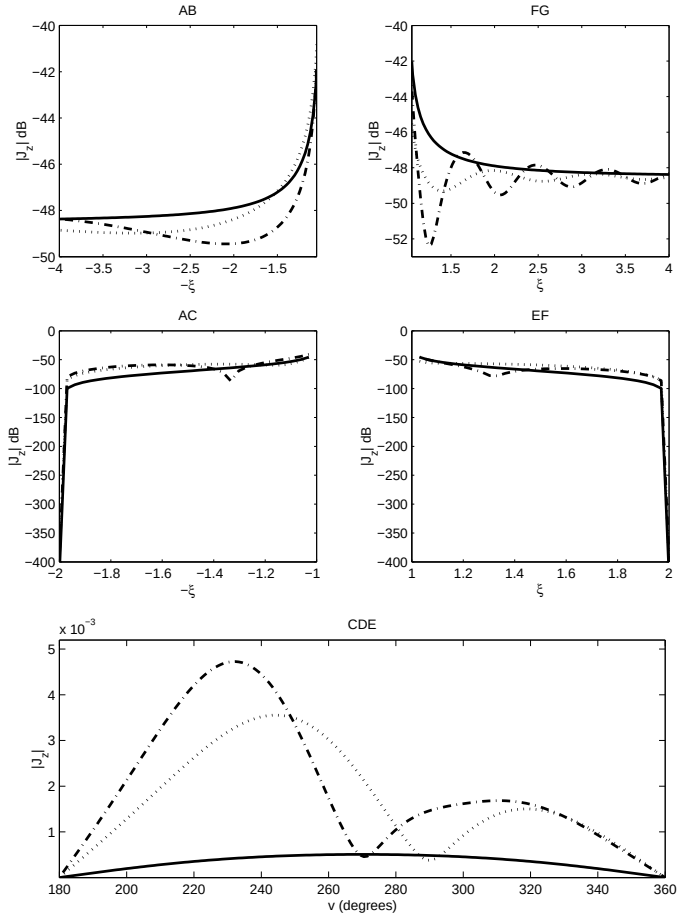

Fig. 4. Induced current for a TM plane wave incident at $\varphi_0 = \pi/4$, with $Z_1 = 120\pi\,\Omega$ and $Z_2 = 120\pi\,\Omega$. Solid line: c=0.1; dotted line c=π, dash-dot line c=4.5

The known equivalent currents M_x and J_z are represented as piecewise-linear functions and equations (17) and (23) are evaluated to obtain values for the total magnetic field. The results are substituted into equations (15), (16), (21), and (22) to obtain the actual currents present on the original structure.

C. Scatterer Method (TM Excitation)

The scatterer method integral equation is solved for the equivalent current on the structure of Fig. 1 [5], which serves as a basis for checking results obtained by other methods. In this method one assumes that the finite groundplane scatterer method of [2] has been employed to determine values for the equivalent current J_z of Fig. 3. In Fig. 3 the endpoints of the aperture are x_1 and x_2, C_s is the contour of the channel backing and the finite width groundplane, J_z is the equivalent electric current on contour C_s, and I is the impressed electric line source.

¿From knowledge of the equivalent current J_z, one can determine the magnetic field everywhere and therefrom compute actual surface currents. The equivalent currents on the surface of the ground plane in region 1 along BC and EG are identical to the actual currents on these surfaces in the original configuration of Fig. 1. The equivalent current on the surface CDE is also the same as the current that exists on the interior-region surface of the PEC elliptic backing of Fig. 1 for an infinitely wide ground plane. However, the currents may differ slightly from the actual currents on this surface for the case of a finite-width ground plane that is assumed in the scatterer method model. If the ground plane is not wide relative to the wavelength, a nonzero field would exist in the lower half-space outside of the ellipse $\xi = \xi_1$ so the equivalent current would not have the same value as the total tangential magnetic field on the interior surface of the ellipse. An explicit statement of this is given in (25), where the equivalent and actual currents are seen to be equal only if

$$H_l^2\left(x,y\right)\big|_{(x,y)\in\xi_1^+} = 0. \tag{26}$$

The equivalent current on the surfaces CA and FE in the scatterer method are the sums of the actual currents present on either side of these baffles in the original configuration. These equivalent currents are used to validate the results obtained from calculating the actual surface currents by means of the coupled integral equation method. The currents are related by

$$\mathbf{J}_z^{scat}\big|_{CA} = J_z\left(x,0^+\right)\big|_{x\in CA} + J_z\left(x,0^-\right)\big|_{x\in CA} \tag{27}$$

where J_z^{scat} is the equivalent electric current on CA obtained from the scatterer method, and $J_z\left(x,0^+\right)|_{x\in CA}$ and $J_z\left(x,0^-\right)|_{x\in CA}$ are the actual currents on the upper and lower surfaces, respectively, which can be computed from the upper and lower surface magnetic fields as described in Section II-B. Similarly, the currents on FE can be related to the equivalent currents of the scatterer method by

$$\mathbf{J}_z^{scat}\big|_{FE} = J_z\left(x,0^+\right)\big|_{x\in FE} + J_z\left(x,0^-\right)\big|_{x\in FE}. \tag{28}$$

III. NUMERICAL COMPARISONS

Data obtained from the analytic solutions of [1] are compared with those of the integral equation methods of Section II by superimposing the results obtained from the two methods. In all cases considered, the semielliptical cavity is located at the elliptic coordinate $\xi_1 = 2$. Figs. 4, 5, 6 show the currents induced along the metallic surfaces of the structure of Fig. 1, which are the ground plane surfaces AB and FG in region 1, the ground plane surfaces AC and EF in region 2, and the semielliptical wall CDE. Each graph displays the total current induced on the surface examined for three different values of the dimensionless quantity $c = kd/2$: $c = 0.1, \pi, 4.5$. Each value of c is identified by a line style for all plotted data, *e.g.*, all results pertaining to $c = 0.1$ correspond to a solid line.

Results for various values of the intrinsic impedances are presented. In particular, the analytic solutions indicate that the modal coefficients of the field expansions depend upon the properties of the isorefractive media through the ratio $\zeta = Z_1/Z_2$. However, for TM polarization,

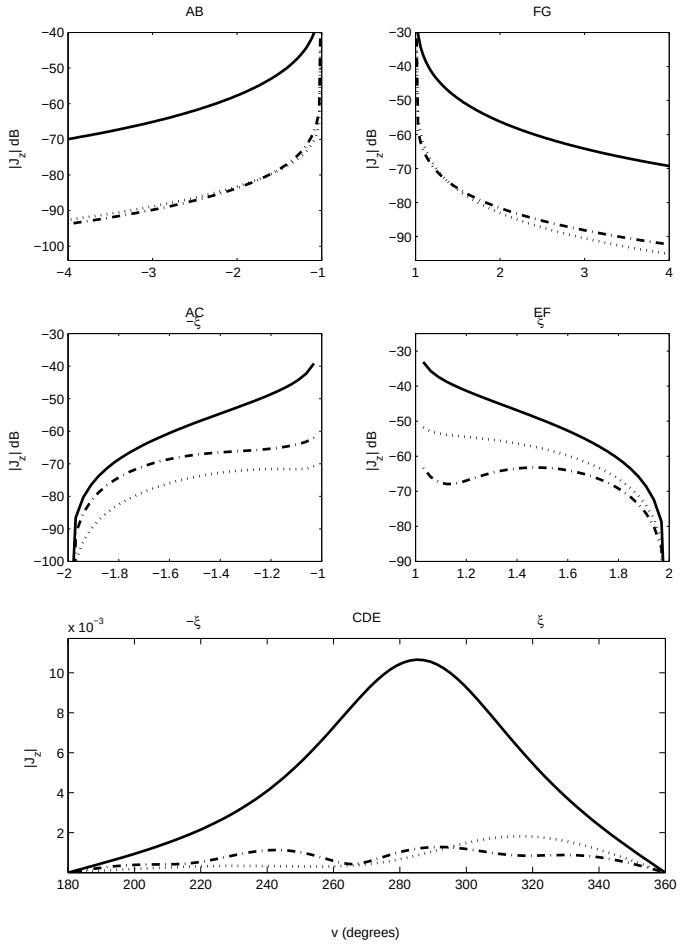

Fig. 5. Induced current for a TM line source located inside the cavity at ($\xi_0 = 1.2, v_0 = -5/12\pi$), with $Z_1 = 120\pi\,\Omega, Z_2 = 240\pi\,\Omega$. Solid line: c=0.1; dotted line c=π, dash-dot line c=4.5

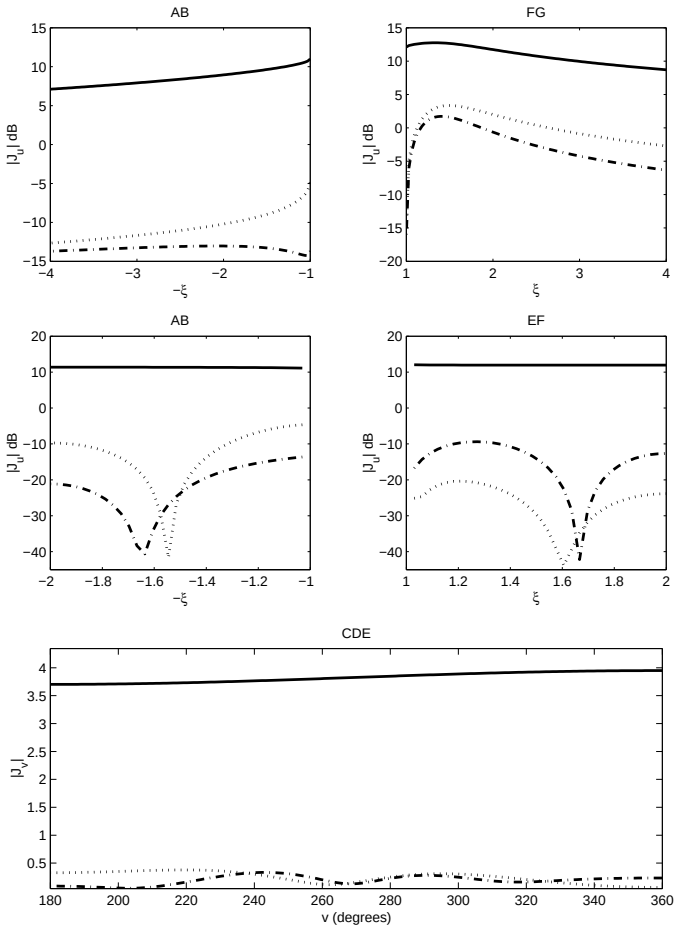

Fig. 6. Induced current for a TE line source located outside the cavity at ($\xi_0 = 1.5, v = \pi/6$), with $Z_1/Z_2 = 2$. Solid line: c=0.1; dotted line c=π, dash-dot line c=4.5

the induced currents depend directly upon the intrinsic impedance of the medium, so that a variation of Z_1 and Z_2 such that ζ is constant will modify the induced current.

The evaluation of the analytical series containing Mathieu functions is carried out using the acceleration technique described in [3]. As a result, usually only 20 terms are evaluated to approximate the sum of any series, with a couple of exceptions where the number of terms considered approaches 40. Approximately 20 pulses per wavelength were used in evaluating the currents via the integral equation methods of Section II.

Fig. 4 shows the total currents present on the structure of Fig. 1 due to a TM-polarized plane wave whose direction of propagation makes an angle $\varphi_0 = \pi/4$ with the negative direction of the x-axis. The integral equations discussed in Section II are evaluated and the results are plotted with those obtained from the analytic formulas (21-23) of [1].

Similarly, Fig. 5 shows the total currents computed for the case of an electric line source located in region 1 at the elliptic coordinates ($\xi_0 = 1.5, v_0 = -5/12\pi$) when $Z_1 = 120\pi\Omega$ and $Z_2 = 240\pi\Omega$. Equations (59-61) of [1] are evaluated and the results are plotted along with those of the integral equation method.

Finally, Fig. 6 displays the total currents for a magnetic line source located in region 1 at the elliptic coordinates ($\xi_0 = 1.5, v_0 = \pi/6$) when $\zeta = 2$. These results are obtained from formulas (66-68) of [1].

The last two figures show the bistatic radar cross section (RCS) of the system shown in Fig. 1. Fig. 7 shows the RCS for TM polarization computed using (16) of [1] and the TM coupled integral equation method. Fig. 8 shows the RCS for TE polarization computed using (29) of [1] and the TE coupled integral equation method.

IV. CONCLUSIONS

The numerical results obtained from the IE method of Section II and the analytic formulas of [1] agree for all the cases examined in Section III and shown in Figs. 4-8. The mutual validation of these methods through computing the currents present along the surfaces of the structure of Fig. 1 provides a new canonical example that involves a cavity, different media, and sharp edges.

Acknowledgments

The authors are grateful to the Reviewers for their useful suggestions.

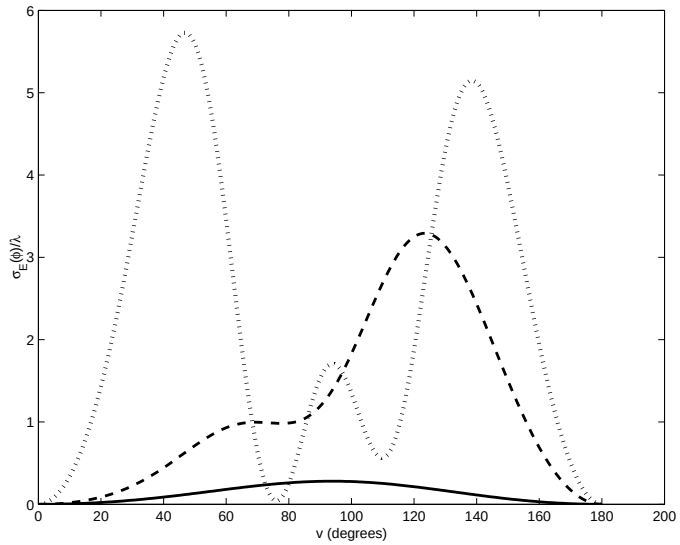

Fig. 7. Bistatic radar cross section for a TM-polarized plane wave incident at an angle $\varphi_0 = \pi/6$ when $Z_1 = 120\pi\,\Omega$ and $Z_2 = 120\pi\,\Omega$. Solid line: c=1; dotted line c=π, dash-dot line c=4.5

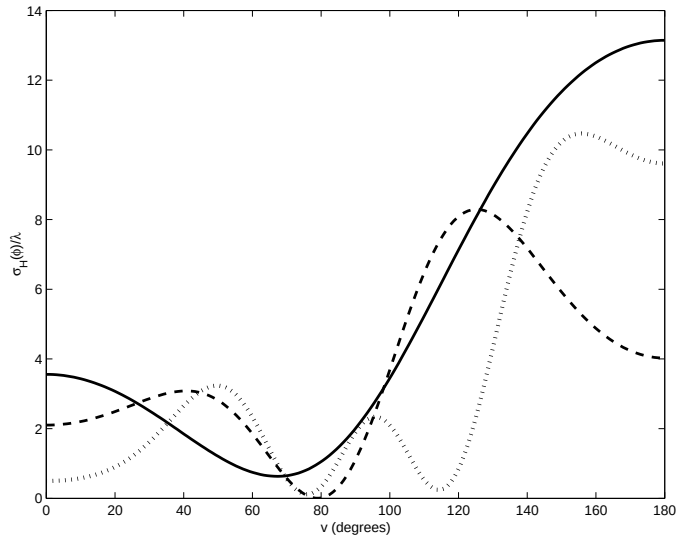

Fig. 8. Bistatic radar cross section for a TE-polarized plane wave incident at an angle $\varphi_0 = \pi/6$ when $Z_1 = 120\pi\,\Omega$ and $Z_2 = 120\pi\,\Omega$. Solid line: c=1; dotted line c=π, dash-dot line c=4.5

References

[1] P.L.E. Uslenghi, "Exact penetration, radiation and scattering for a slotted semielliptical channel filled with isorefractive material," *IEEE Trans. Antennas Propagat.*, vol. 52, no. 6, pp. 1473–1480, June 2004.

[2] D. Erricolo, M. D. Lockard, C. M. Butler, and P.L.E. Uslenghi, "Numerical analysis of penetration, radiation and scattering for a 2D slotted semielliptical channel filled with isorefractive material," *PIER*, accepted.

[3] D. Erricolo, "Acceleration of the convergence of series containing Mathieu functions using Shanks transformation," *IEEE Antennas and Wireless Propagation Letters*, vol. 2, no. 1, pp. 58–61, 2003.

[4] J. D. Shumpert and C. M. Butler, "Penetration through slots in conducting cylinders: Part 1, te case, analysis of a strip in a waveguide," *IEEE Trans. Antennas Propagat.*, vol. 46, no. 11, pp. 1612–1621, November 1998.

[5] C. M. Butler, "Investigation of a scatterer coupled to an aperture in a conducting screen," *Proc. IEE*, vol. 127, Pt. H, no. 3, pp. 161–169, June 1980.